Geophysical Research Letters

RESEARCH LETTER
10.1029/2018GL079168

Key Points:
- The 1-km-resolution model broadly reproduces the restricted and nonuniform glaciation over HMA in the LGM
- The climate sensitivity of glaciers across HMA shows high region variability in glaciation
- Insufficient cooling and/or precipitation decrease constrained glaciation over HMA in the LGM, but the dominant factor is region dependent

Supporting Information:
- Supporting Information S1

Correspondence to:
Q. Yan,
yanqing@mail.iap.ac.cn

Citation:
Yan, Q., Owen, L. A., Wang, H., & Zhang, Z. (2018). Climate constraints on glaciation over High-Mountain Asia during the last glacial maximum. *Geophysical Research Letters*, *45*, 9024–9033. https://doi.org/10.1029/2018GL079168

Received 10 JUN 2018
Accepted 12 AUG 2018
Accepted article online 24 AUG 2018
Published online 6 SEP 2018

Climate Constraints on Glaciation Over High-Mountain Asia During the Last Glacial Maximum

Qing Yan[1,2], Lewis A. Owen[3], Huijun Wang[2], and Zhongshi Zhang[4,5]

[1]Nansen-Zhu International Research Centre, Institute of Atmospheric Physics, Chinese Academy of Sciences, Beijing, China, [2]Key Laboratory of Meteorological Disaster/Collaborative Innovation Center on Forecast and Evaluation of Meteorological Disasters, Nanjing University of Information Science and Technology, Nanjing, China, [3]Department of Geology, University of Cincinnati, Cincinnati, OH, USA, [4]Department of Atmospheric Science, School of Environmental Studies, China University of Geosciences, Wuhan, China, [5]Uni Research Climate, Bjerknes Center for Climate Research, Bergen, Norway

Abstract Reasons for restricted and nonuniform glaciation over High-Mountain Asia (HMA) during the global last glacial maximum (LGM; ~28-23 ka) have been intensively studied but remain elusive. Using a 1-km-resolution ice sheet model, we show that glaciers across HMA exhibit high region variability in glaciation. Glaciers in western and southern HMA are the most sensitive to climate change and those in the interior are the least sensitive. Our model broadly reproduces the restricted glaciation across HMA during the LGM, although it overestimates the extent of glaciation over western and southern HMA as compared with reconstructions. Modeled decreases in precipitation hampers glacier growth over northern HMA, while insufficient cooling hampers glacier advance over eastern HMA for the LGM. Both reduced precipitation and insufficient cooling inhibit large-scale glaciation over inner HMA. Moreover, climatic conditions conducive to glaciation across the entire HMA include a reduction in temperature of ~10 °C and an increase in precipitation, unlikely to have occurred during any Quaternary glacial maximum.

Plain Language Summary Presently, High-Mountain Asia (HMA) is home to the largest mass of glaciers outside the polar regions and known as the Earth's Third Pole. During the global last glacial maximum (LGM; ~28–23 ka), geological evidence points to restricted and nonuniform glaciation over HMA, in stark contrast to the expanded ice sheets across high latitudes of Northern Hemisphere. However, it remains elusive why was there no large-scale ice sheet over HMA during the LGM. Using a 1-km-resolution ice sheet model, we highlight the climate sensitivity of glaciers across HMA showing highly region variability in glaciation and revealing that insufficient cooling and/or precipitation decrease constrained glaciation over HMA during the LGM.

1. Introduction

High-Mountain Asia (HMA) is a vast area stretching ~2,000 km east-west by 1,500 km north-south containing major mountain ranges that include the Greater Himalaya, Karakoram, Pamir, Kunlun Shan, and Tien Shan. The average elevation across the Himalaya and Tibet is ~5,000 m above sea level. This dramatic topographic relief makes HMA very cold given its relatively low latitude. The South Asian monsoon and midlatitude westerlies advect moisture into HMA, much of which falls as snow at high altitudes that helps sustain the largest mass of glaciers outside the polar regions (Benn & Owen, 1998; Yao, Thompson, Mosbrugger, et al., 2012). As such, HMA has also become known as Earth's Third Pole (Yao, Thompson, Yang, et al., 2012). Future glacier fluctuations in HMA will have a profound effect on water availability, biodiversity, and the livelihoods of hundreds of millions of people across Asia (Xu et al., 2009). Determining the factors that drive past and present, and hence future glaciation in HMA, therefore, has important socioeconomic implications for assessing the impacts of future climate and environmental change in the region.

Kuhle (e.g., Kuhle, 1985, 1998) argued that an extensive ice sheet (~2–2.4 × 10^6 km^2) developed over HMA during the global last glacial maximum (LGM) at ~28–23 ka (Hughes & Gibbard, 2015), somewhat similar to the expanded ice sheets across the high latitudes of the Northern Hemisphere (Dyke et al., 2002). This was based largely on his studies during field expeditions and equilibrium-line altitude reconstructions. This view, however, was very contentious and stimulated much glacial geologic research that presented evidence to show that an ice sheet did not have existed over Tibet (e.g., Owen & Dortch, 2014, and references therein). In particular, in extensive areas of HMA, terrestrial cosmogenic nuclide exposure dating showed that numerous moraines relatively close to present ice caps and glaciers formed during the penultimate glacial cycle or much earlier, hence providing evidence that a large ice sheet did not exist otherwise the moraines would not have been preserved (e.g., Heyman, 2014; Owen et al., 2002; Owen & Dortch, 2014; Seong et al., 2007). Overall, the abundant glacial geological evidence and numerical dating against the ice sheet hypothesis points to restricted extent of glaciation over HMA during the LGM. As such, two important questions arise: (1) Why was there not a large-scale ice sheet over HMA during the LGM? and (2) Under what climatic conditions might an extensive ice sheet develop over HMA?

Although considerable efforts have been made to help answer these questions (e.g., Bintanja et al., 2002; Jiang et al., 2004; Kirchner et al., 2011; Liu et al., 2002), the dearth of paleoclimate proxy data sets and a poor understanding of glacier response to climate perturbations across HMA has hindered any satisfactory explanations of the nature and pattern of glaciation during the LGM. To help address these questions, we used the Parallel Ice Sheet Model (PISM) with a horizontal resolution of 1 km by quantifying the climate sensitivity of the glaciers and exploring potential mechanisms and driving factors for HMA glaciation during glacial conditions. We focused on the variation of glacier extent because of very limited knowledge on ice volume/thickness over HMA for the LGM. In particular, our study aims to provide insights into the paleoglaciological history of HMA and helps advance knowledge of the relationship between climate change and glacier behavior.

2. Methodology

2.1. Ice Sheet Model

The PISM is a three-dimensional, thermodynamically coupled ice sheet model (Bueler & Brown, 2009; Winkelmann et al., 2011) that has been widely used to compute the evolution of ice sheets and glaciers under past and future climates (e.g., Golledge et al., 2012, 2015). In brief, in the model, surface mass balance depends on the monthly air temperature and precipitation, with an empirical relation to partition precipitation into rainfall and snowfall and a positive-degree day scheme to estimate ablation. The PISM adopts a hybrid stress balance model that combines shallow ice and shallow shelf approximations to calculate ice flow. A pseudo-plastic power law is used to compute basal sliding. In our study, the PISM is run at a horizontal resolution of 1 km over the entire HMA using 3,200 × 2,000 grid points, and the present-day topography is derived from global multiresolution terrain elevation data of 2010 (Danielson & Gesch, 2011). A list of ice sheet model parameters that are used in our simulations is given in Table S1.

The PISM has proven to be very effective for depicting ice flows and mass balance for ice sheets and ice caps (Aschwanden et al., 2016; Jouvet et al., 2017), but may not be suitable for smaller valley glaciers due to their size, geometry, hypsometry, debris cover, and slope variability. Hence, this places some limitations on the shallow ice + shallow shelf approximation hybrid approach and positive-degree day method. Our study incorporates ice sheets, ice caps, and valley glaciers, especially during the LGM, so that the PISM represents glaciers in certain areas better than others. However, even at 1-km resolution there is still uncertainty in the representation of small valley glaciers.

2.2. Climatic Forcing

We selected four temperature and six precipitation data sets for the present day. Briefly, the four modern temperature fields include the ERA-Interim Reanalysis of Dee et al. (2011), the High Asia Reanalysis of Maussion et al. (2014), the Climatic Research Unit of Harris et al. (2014), and the WorldClim of Hijmans et al. (2005; Figure S1). In addition to the four data sets, the modern precipitation field includes two data sets from the Asian Precipitation-Highly-Resolved Observational Data Integration Towards Evaluation of the Water Resources (Yatagai et al., 2012) and the Tropical Rainfall Measuring Mission (Huffman et al., 2007; Figure S2). We then combined each temperature and precipitation data set to construct 24 sets of present-day climatic forcing (Text S1) because each data set may have its own advantages and disadvantages over HMA.

We used the model output (monthly temperature and precipitation) from the Paleoclimate Modeling Intercomparison Project phases II and III for the LGM (PMIP; Braconnot et al., 2011; Table S2). We first calculated the simulated temperature anomalies and precipitation ratios between the LGM and the baseline experiments from individual climate models, and then computed the multimodel ensemble mean. Next, these anomalies were interpolated to 1-km resolution and then added to the present-day climatic fields that are used in the PISM to generate the LGM climatic forcing.

2.3. Experimental Design

We first ran the PISM at 10-km resolution for 20,000 years to reach quasi-equilibrium with climate forcing fixed at the present day to simulate modern glaciers over HMA. The experiment was then refined to 5 km for another 5,000 years, to 2 km for 500 years, and finally to 1 km for 50 years for computational efficiency (Aschwanden et al., 2016).

Stepwise change (at 1 °C increments) in temperature from −1 to −10 °C was uniformly added to the present-day climatic field over HMA with no change in precipitation to study the role of temperature in glacier extent. Similarly, precipitation was uniformly increased from 25 to 1,000% with uneven intervals (i.e., +25, +50, +75, +100, +200, +300, +400, +500, +750, and +1,000%) over HMA with temperature unchanged to examine the influence of precipitation. Furthermore, we added an incremental temperature change of 1 °C from −1 to −10 °C to the present-day climatic field together with precipitation perturbated of +50, +25, −25, and −50%, respectively, to examine the glacier response to different combinations of temperature and precipitation forcings. Starting from the modeled present-day HMA glaciers, each of these experiments was integrated for 4,500 years on a 5-km grid, and refined to 2 km for 450 years and to 1 km for 50 years.

To simulate glacier extent during the LGM, the model was initialized from the present-day simulation and is ran for 5,000 years on a 1-km grid forced by the created LGM climatic forcings from PMIP2 and 3 (i.e., "steady state" run). Next, we performed a set of idealized sensitivity experiments to estimate the relative importance of temperature and precipitation change in forcing glaciation. Specifically, we repeated the LGM experiment with precipitation fixed at the present day and increased by 50%, and with additional temperature reduction of −5 °C.

2.4. Model-Data Comparisons for Climate Change During the LGM

We compiled available proxies over HMA that provide quantitative information for temperature and precipitation during the LGM (Tables S3 and S4). These proxies suggest a cooling of ~2–9 °C and ~33–68% less precipitation relative to the present day over HMA during the LGM. At the simplest case, averaging all the proxies yielded a decrease of temperature and precipitation by ~6 °C and 51% over HMA, respectively. The PMIP3 models predict a decrease of annual mean temperature by ~5 °C during the LGM, with the most intense cooling occurring at western and southern HMA (Figure S3). Regionally averaged annual mean precipitation over HMA decreases by ~57%, and the magnitude of precipitation reduction generally increases with latitude. The PMIP2 models produce a similar anomaly pattern for the LGM, with a decrease of temperature and precipitation by ~5 °C and 51%, respectively. Given the uncertainty in paleoclimate proxies and dating, the model results are broadly consistent with the reconstructions, although regional discrepancy still exits (Figure S3).

3. Results

3.1. Modeling the Distribution of Present-Day Glaciers

A precondition for reconstructing past glacier responses to climate change is that the ice sheet model must largely captures the modern glacier distribution over HMA. This proves challenging due to the uncertainty in the present-day climatic forcing and the low-resolution of the models used in previous studies (Kirchner et al., 2011). Therefore, we ran the 1-km-resolution PISM with various climatic fields (totally 24 sets; Text S1), and then optimized the present-day climatic forcing by evaluating the model performance in depicting glacier extent given relatively larger uncertainty and limited information on ice thickness/volume and velocity.

The extent of the modeled modern glaciers over HMA varies greatly with the climatic forcing (CF). The simulated total glacier area (TGA) is ~3 times larger than the observations (Randolph Glacier Inventory 6.0; RGI Consortium, 2017) in response to CF1, CF2, CF7, and CF8 (Figure 1a). In contrast, the model predicts far fewer glaciers over HMA when forced by CF21–24. This leads to an underestimation of the TGA by >75% (Figure 1a). With respect to the remaining climatic forcings, the observed glacier area over western HMA is underestimated by >75% in the simulations with the climatic fields from CF15–18 (Figure 1b), partly arising from unresolved glaciers over the Karakoram (Figure S4). The PISM captures the glacier distribution over southern HMA (e.g., along the Himalaya) but broadly overestimates the glacier area, whereas the number of glaciers over Tien Shan is underestimated (Figures 1b, S5, and S6). However, each climatic forcing has its

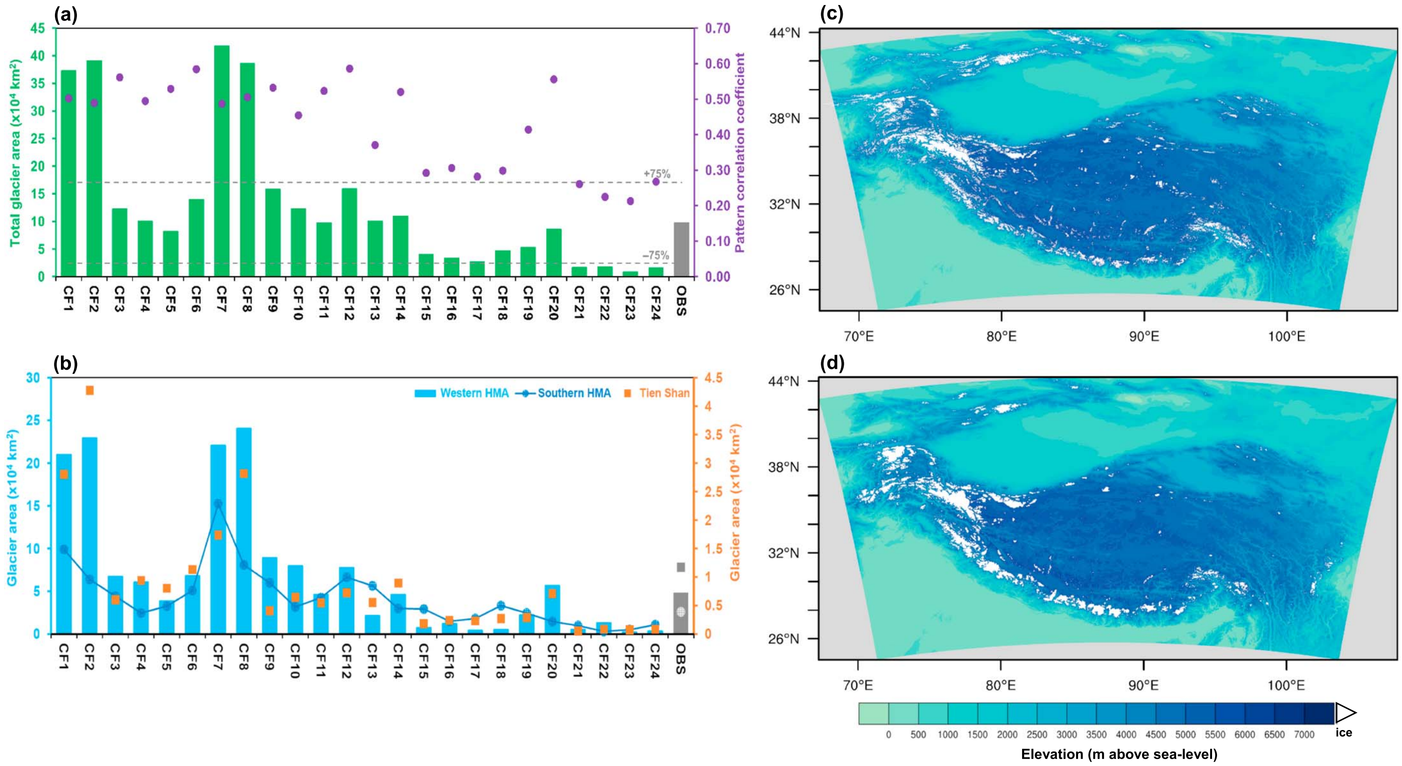

Figure 1. Total present-day glaciated area over HMA. (a) Modeled TGA (bars) with different present-day climatic forcings and pattern correlation coefficient (dots) in glaciated grids between simulations and observations. The gray dash lines show the TGA that is 75% larger/smaller than the observations (gray bar). (b) Modeled glaciated area over three subregions of HMA (see Figure S20 for definition). Modern glacier distribution in (c) observations and (d) simulation with CF12 (ice thickness > 10 m).

own strengths and weaknesses, and a match in the glaciated area does not necessarily guarantee spatial similarity with present-day reality. To select the "most suitable" present-day forcing, we estimated the pattern correlation in glaciated grids between the simulations and the observations (Figure 1a and Text S2). CF12 (temperature from High Asia Reanalysis and precipitation from Tropical Rainfall Measuring Mission; Figure S7) stood out as being the most similar.

The modeled glacier distribution over HMA closely resembles observations in response to CF12 (Figures 1c and 1d). The majority of glaciers are located at the western end of HMA, the Himalaya, the south-eastern Tibetan Plateau, and Tien Shan, with fewer glaciers in the interior of HMA and parts of northern and eastern HMA. However, the model still misses a number of small-scale glaciers mainly over northern HMA and Tien Shan (by ~40% in glacier area). Whereas, the model overestimates the TGA by ~60%. This partly arises from the uncertainty in climatic fields over western HMA and the Himalaya where the observations are sparse. Additionally, we explored the effect of model resolution on the simulated glaciers. The model with a resolution of ≤5 km roughly captures the observed glacier distribution over HMA (Figure S8). Higher model resolution yields a closer match with the glacier distribution due to the greater number of resolved glaciers.

3.2. Glacier Sensitivity to Temperature and Precipitation

To examine the influence of temperature on glacier growth, stepwise temperature perturbations from −1 to −10 °C were applied uniformly over HMA in 1 °C increments, keeping precipitation unchanged. In response to a cooling of 1–4 °C, glacier expansion is mainly observed over western and southern HMA and the Tien Shan, with a TGA of ~81.2 × 10^4 km^2 (Figures 2a, 2c, and S9). With further temperature reductions of 5–8 °C, glaciers begin to develop over eastern and northern HMA and the TGA increases to ~237.1 × 10^4 km^2. Driven by 9–10 °C temperature depressions, the model predicts an extensive ice sheet over HMA, with the TGA increasing to ~284.8 × 10^4 km^2, that is, ~17 times more extensive than the present-day glacier cover. The interior and low-elevation areas surrounding HMA are the last places to experience

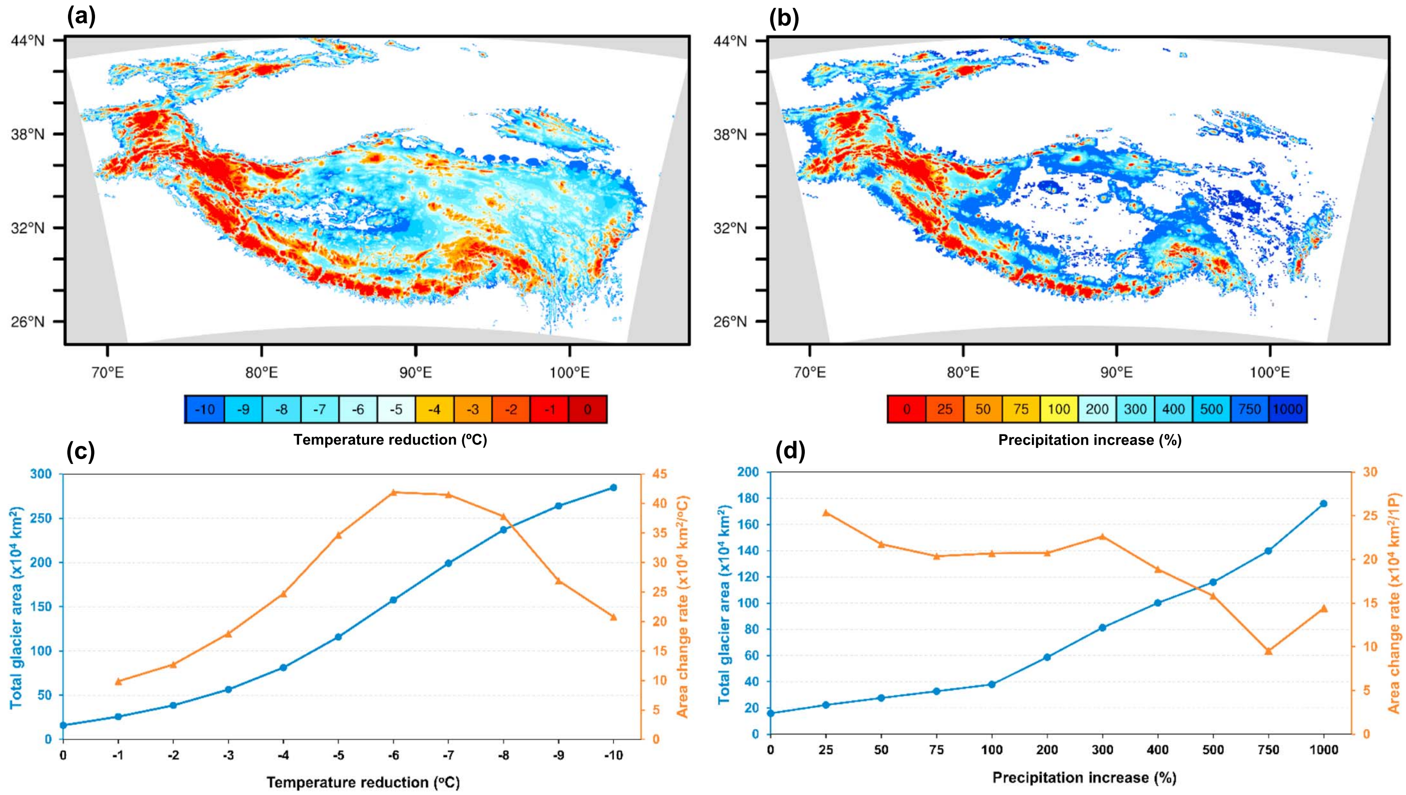

Figure 2. Sensitivity of glacier extent to temperature and precipitation perturbations. (a) The lowest temperature reduction (°C) required for glaciation over each grid with no change in precipitation. (b) The smallest percentage precipitation increase required for glaciation with no change in temperature. Blank areas indicate that there is no glaciation when temperature is decreased by 10 °C or precipitation is enhanced by 1,000%. Glacier extent in response to a certain temperature/precipitation anomaly (Δx) includes all the areas with temperature/precipitation anomaly $\leq \Delta x$. TGA and its change rate in response to (c) stepwise (1 °C) temperature perturbations from -1 to -10 °C and (d) precipitation perturbations of 25–1,000% in uneven increments.

glaciation due to their extreme aridity and higher air temperature, respectively (Figure S10). Additionally, the total glacier volume (TGV) increases by ~2–58 times with an equivalent sea level drop of 0.2–6.4 m in response to a cooling of from 1 to 10 °C (Table S5).

Precipitation amounts were uniformly increased by 25 to 1,000% in uneven increments, this time keeping temperature fixed, to investigate the influence of precipitation on glacier extent. When forced by a doubling of present-day precipitation values across HMA, the model predicts an increase of the TGA (TGV) by ~1.4 (3.1) times to 40.0×10^4 km^2 (0.34 m; Figures 2b and 2d and Table S5), with glacier expansion mainly occurring over western and southern HMA (Figure S11). With precipitation from 3 to 6 times greater than present, glaciers further develop over western and southern HMA and the Tien Shan, with a TGA (TGV) of ~116.1×10^4 km^2 (1.7 m). However, a plateau-wide ice sheet still does not completely form over HMA even when the precipitation was increased by 750–1,000%, especially over the interior and eastern end of HMA. This is likely because the increased snowfall cannot adequately compensate for the rates of surface ablation.

In general, our results indicate an increase of the TGA by ~9.9×10^4 to 268.9×10^4 km^2 in response to temperature reductions from -1 to -10 °C, and by ~6.3×10^4 to 160×10^4 km^2 with precipitation perturbations of 25–1,000%. The rate of change in the TGA exhibits a concave-down pattern (peaking at -6 °C) with the imposed decreasing temperatures, but falls with increasing precipitation (Figures 2c and 2d) and shows high region variability (Figure S12). On average, the model predicts an increase of the TGA by ~26.7×10^4 km^2 (1.7 times the present glaciated area) for every 1 °C of cooling and by ~19.0×10^4 km^2 (~1.2 times) for every doubling in precipitation. Glaciers in western and southern HMA are the most sensitive to climate perturbations and glaciers in the interior appear to be the least sensitive (Figures 2a and 2b). This variation in glacier sensitivity is largely attributed to the difference in the background climate state, which is broadly colder and/or wetter in western and southern HMA than the interior (Figure S7).

10.1029/2018GL079168

3.3. Glacier Expansion Under Glacial Climates

Given the sparseness of paleoclimate proxy records for the LGM across HMA, we first investigated glacier growth under a set of idealized glacial climates. In response to a cooling of 6 °C and a precipitation decrease of 50%, as estimated by multiproxies (section 2.4), glaciation is mainly concentrated in western and southern HMA and the Tien Shan, with a TGA (TGV) of 79.3×10^4 km^2 (0.6 m; Figure 3a). In contrast, an extensive ice sheet (217.5×10^4 km^2) develops over much of HMA except for the interior if precipitation is increased by 50% (Figure 3b). This is attributed to the fact that enhanced precipitation provides more favorable conditions, that is, increased accumulation, for glaciation with the same reduction in temperature. Glaciation over the entire HMA is achieved with a 10 °C cooling and a 50% increase in precipitation (Figure 3d), and the TGV reaches ~8.7 m, while the interior remains largely ice-free in response to a decrease in temperature of 10 °C with reduced precipitation (Figure 3c). In addition, for a given precipitation perturbation, varying drops in temperature are needed for glacier growth, depending on the region. The interior requires the greatest temperature drop, the north and east less, and the western and southern HMA the least (Figure S13). This regional heterogeneity results from the difference in present-day precipitation (Figure S7). The western and southern HMA receives enough snowfall to be glaciated, whereas the interior HMA experiences extreme aridity and hence requires greater temperature reduction for glaciation.

Furthermore, we examined the response of glaciers to a more realistic scenario for the LGM using the PMIP3 models. Under the simulated colder and drier climate, the TGA increases by ~4.1 times that of the modeled present glacier cover, to 80.8×10^4 km^2 for the LGM, and the TGV corresponds to a rise of global sea level by ~0.86 m. Glaciers expand significantly and grow into ice caps over western and southern HMA, and extensive valley glaciers form over parts of eastern and northern HMA (Figure 4a). However, large-scale glaciation still barely occurs over the interior of HMA. This reconstruction of glacier distribution is insensitive to the LGM forcing, since it is also observed in our experiment that takes the climatic forcing from the PMIP2 models (Figure S14). Although the values of ice sheet model parameters are poorly constrained and they may change under different environmental conditions, the restricted glacial expansion and ice-free conditions in the interior of HMA are independent of the selected PISM parameters (Figure S15 and Text S3).

The modeled LGM glacier extent is broadly consistent with the geologic reconstructions. Glacial geologic data and equilibrium-line altitude reconstructions show that parts of western and southern HMA experienced extensive glacier advances during the LGM (e.g., Seong et al., 2007; Eugster et al., 2016; Figure S16 and Table S6), whereas glaciation was less extensive in other parts of the two regions (e.g., Amidon et al., 2013). Additionally, there was very limited glacier advance over the interior and northern HMA during the LGM (Heyman, 2014; Owen et al., 2002; Owen & Dortch, 2014; Shi, 2002). Quantitatively, the modeled fourfold increase in the TGA is larger than the reconstructions that estimate an increase of the TGA by ~3 times (Shi, 2002). This model-data discrepancy may be partially attributed to the limitations of the positive-degree day method and missing processes in climate/ice sheet models, as well as uncertainties in present-day and LGM climates.

We then explored which factors, including insufficient cooling, decreased precipitation, or both, inhibit large-scale glaciation across HMA for the LGM in our simulations. Sensitivity experiments show that the cooling in the LGM alone could lead to the additional formation of ice caps over the central Kunlun Shan and parts of central HMA, when compared to the LGM experiment, as well as enhanced glaciation over the Tien Shan and Qilian Shan (Figures 4 and S17). This result may be indicative of the important role of precipitation reduction in constraining glacier growth over these regions. However, the possibility that there has been insufficient cooling over northern HMA cannot be fully excluded given the uncertainties in climate model and reconstructions. The interior of HMA remains ice-free even if the modeled LGM cooling is accompanied by a 50% increase in precipitation, or if an additional cooling (−5 °C) is added to the LGM climate (Figure 4). The interior can become fully glaciated with a decrease in temperature of 10 °C in tandem with an increase in precipitation (Figure 3d). Thus, both insufficient cooling and decreased precipitation hamper glacier expansion over the interior of HMA for the LGM. Eastern HMA experiences large-scale glaciation during the LGM, likely in response to enhanced LGM cooling, while the modeled LGM temperature reduction with a 50% increase in precipitation is only favorable for the development of extensive valley glaciers and ice caps, but not large-scale ice sheet growth (Figures 4 and S17). This suggests that insufficient cooling plays a dominant role in preventing ice sheet formation over eastern HMA.

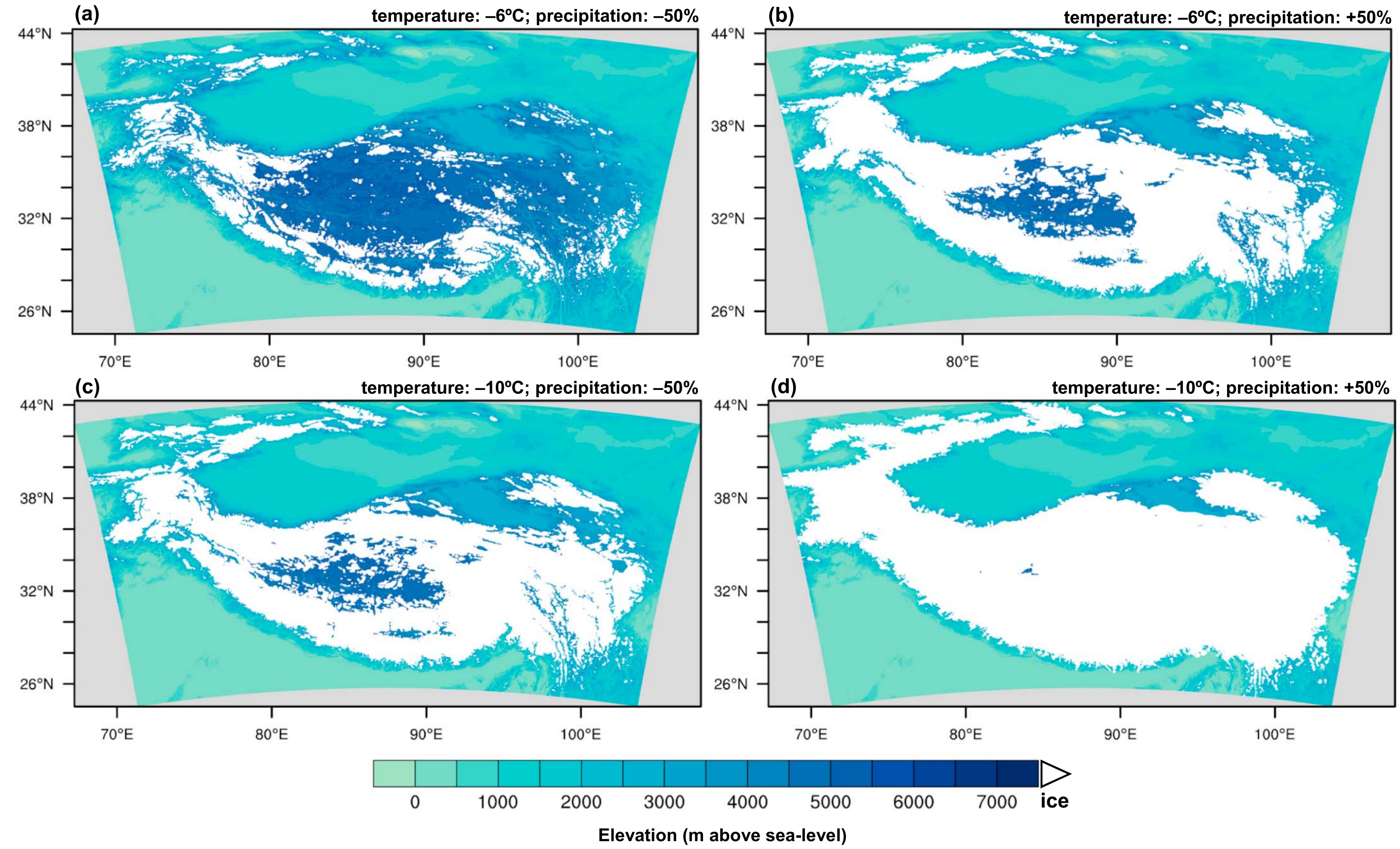

Figure 3. Glacier extent under idealized glacial climates. The modeled glacier distribution in response to temperature reductions of (a and b) −6 °C and (c and d) −10 °C with precipitation perturbations of (a and c) −50% and (b and d) +50%.

4. Conclusions

Our results indicate that the climate sensitivity of glaciers across HMA is highly region-dependent, with glaciers in western and southern HMA being the most sensitive, and those in the interior being the least sensitive. Our model broadly captures the restricted glacier expansion over HMA during the LGM as suggested by the geologic evidence, although it produces too extensive glaciation over western and southern HMA. We provide possible answers for the two questions raised at the outset: (1) the lack of a plateau-scale ice sheet over HMA during the LGM is likely the result of the important role of climate in constraining glaciation over HMA during the LGM, although the dominant factor, that is, insufficient cooling or reduced precipitation, varies between different regions and (2) the climatic conditions conducive to large-scale glaciation in HMA include a reduction in temperature of ~10 °C together with an increase in precipitation. However, atmospheric water vapor declines with decreasing temperature, and atmospheric circulation in a cold climate, that is, weaker Asian monsoon (Wang et al., 2005), is generally unfavorable for a precipitation increase over HMA. Thus, we argue, it is likely that little large-scale glaciation could develop across HMA during any Quaternary glacial maximum. However, more geologic proxies for climate change and glacier extent are needed to test this hypothesis.

Efforts have been made to study the glacier development during the LGM over the entire HMA, but they failed to capture the reconstructed alpine-style glaciation (Bintanja et al., 2002; Jiang et al., 2004; Kirchner et al., 2011; Liu et al., 2002). The 1-km-grid PISM broadly reproduces the restricted glacier growth during the LGM, although with overestimated glaciation over western and southern HMA, hence providing additional clues on the climate constraints on glaciation. Insufficient cooling and/or reduced precipitation possibly played an important role in shaping glacier extent during the LGM (e.g., Owen et al., 2005; Owen & Dortch, 2014; Shi, 2002). However, these hypotheses have not been

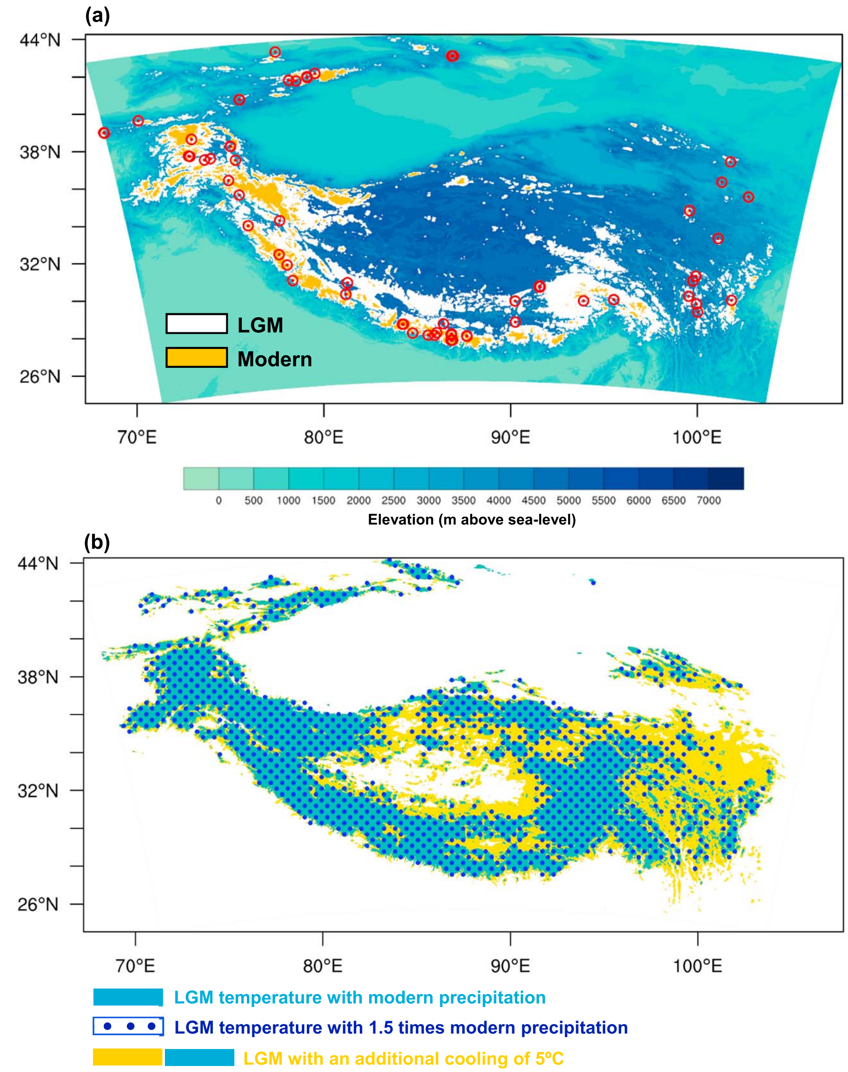

Figure 4. Glacier extent under LGM climates. (a) Modeled glacier distribution in the LGM with PMIP3 forcing. The red dots show the sites where glacier advances have recognized for the LGM over HMA (Table S6). (b) Modeled glacier distribution in response to LGM temperature and present-day precipitation (blue shading), LGM temperature and precipitation with an additional cooling of 5 °C (yellow plus blue shadings), and LGM temperature with 1.5 times present-day precipitation (blue dots).

tested over HMA until now and the relative importance of temperature and precipitation change has remained unclear, except for several individual glacier systems (Heyman, 2010; Xu, 2014). Our results confirm the role of climate in constraining glaciation over HMA and highlight that the dominant factor is region-dependent. Moreover, the modeled regional heterogeneity in glacier response support the findings of glacial geologic studies, based on limited proxies, that spatial patterns in glacier behaviors are expected even if there is a uniform change in forcing (Rupper et al., 2009; Owen & Dortch, 2014).

Although there are several caveats to be considered (Text S4), our study provides a testable relationship between climate change and glacier expansion, potentially shedding light on the paleoglaciological history of HMA. Moreover, the modeled spatial pattern of lowest temperature reduction required for glaciation with different precipitation perturbations (Figure S18) may serve as a possible reference map, together with field evidence, to help define the patterns of paleoclimate change and assess the potential socioeconomic impacts of future climate change scenarios in the region.

Acknowledgments

Many thanks to Jakob Heyman and an anonymous reviewer for their very constructive and useful comments in helping to improve our manuscript. PISM can be downloaded at http://www.pism-docs.org. The PMIP data can be found at https://pmip3.lsce.ipsl.fr/. The PISM outputs are available at https://zenodo.org/record/1319876. This study was supported by the Strategic Priority Research Program of the Chinese Academy of Sciences (XDA20070103), the National Natural Science Foundation of China (41472160), and the Young Elite Scientists Sponsorship Program by CAST (2017QNRC001). Z.S. Zhang thanks the support of Thousand Talents Program for Distinguished Young Scholars.

References

Amidon, W. H., Bookhagen, B., Avouac, J. P., Smith, T., & Rood, D. (2013). Late Pleistocene glacial advances in the western Tibet interior. *Earth and Planetary Science Letters*, *381*, 210–221. https://doi.org/10.1016/j.epsl.2013.08.041

Aschwanden, A., Fahnestock, M. A., & Truffer, M. (2016). Complex Greenland outlet glacier flow captured. *Nature Communications*, *7*, 10524. https://doi.org/10.1038/ncomms10524

Benn, D. I., & Owen, L. A. (1998). The role of the Indian summer monsoon and the mid-latitude westerlies in Himalayan glaciation: Review and speculative discussion. *Journal of the Geological Society*, *155*(2), 353–363. https://doi.org/10.1144/gsjgs.155.2.0353

Bintanja, R., Van de Wal, R. S. W., & Oerlemans, J. (2002). Global ice volume variations through the last glacial cycle simulated by a 3-D ice-dynamical model. *Quaternary International*, *95*, 11–23.

Braconnot, P., Harrison, S. P., Otto-Bliesner, B., Abe-Ouchi, A., Jungclaus, J., & Peterschmitt1, J.-Y. (2011). The paleoclimate modeling Intercomparison project contribution to CMIP5. *CLIVAR Exchanges*, *56*, 15–19.

Bueler, E., & Brown, J. (2009). Shallow shelf approximation as a "sliding law" in a thermomechanically coupled ice sheet model. *Journal of Geophysical Research*, *114*, F03008. https://doi.org/10.1029/2008JF001179

Danielson, J. J., & Gesch, D. B. (2011). Global multi-resolution terrain elevation data 2010 (GMTED2010) (No. 2011–1073). US Geological Survey.

Dee, D. P., Uppala, S. M., Simmons, A. J., Berrisford, P., Poli, P., Kobayashi, S., et al. (2011). The ERA-interim reanalysis: Configuration and performance of the data assimilation system. *Quarterly Journal of the Royal Meteorological Society*, *137*(656), 553–597. https://doi.org/10.1002/qj.828

Dyke, A. S., Andrews, J. T., Clark, P. U., England, J. H., Miller, G. H., Shaw, J., & Veillette, J. J. (2002). The Laurentide and Innuitian ice sheets during the last glacial maximum. *Quaternary Science Reviews*, *21*(1-3), 9–31. https://doi.org/10.1016/S0277-3791(01)00095-6

Eugster, P., Scherler, D., Thiede, R. C., Codilean, A. T., & Strecker, M. R. (2016). Rapid last glacial maximum deglaciation in the Indian Himalaya coeval with midlatitude glaciers: New insights from ^{10}Be-dating of ice-polished bedrock surfaces in the Chandra Valley, NW Himalaya. *Geophysical Research Letters*, *43*, 1589–1597. https://doi.org/10.1002/2015GL066077

Golledge, N. R., Fogwill, C. J., Mackintosh, A. N., & Buckley, K. M. (2012). Dynamics of the last glacial maximum Antarctic ice-sheet and its response to ocean forcing. *Proceedings of the National Academy of Sciences*, *109*(40), 16,052–16,056. https://doi.org/10.1073/pnas.1205385109

Golledge, N. R., Kowalewski, D. E., Naish, T. R., Levy, R. H., Fogwill, C. J., & Gasson, E. G. (2015). The multi-millennial Antarctic commitment to future sea-level rise. *Nature*, *526*(7573), 421–425. https://doi.org/10.1038/nature15706

Harris, I. P. D. J., Jones, P. D., Osborn, T. J., & Lister, D. H. (2014). Updated high-resolution grids of monthly climatic observations—The CRU TS3. 10 dataset. *International Journal of Climatology*, *34*(3), 623–642. https://doi.org/10.1002/joc.3711

Heyman, J. (2010). Palaeoglaciology of the northeastern Tibetan Plateau. Doctoral dissertation. Department of Physical Geography and Quaternary Geology, Stockholm University.

Heyman, J. (2014). Paleoglaciation of the Tibetan plateau and surrounding mountains based on exposure ages and ELA depression estimates. *Quaternary Science Reviews*, *91*, 30–41. https://doi.org/10.1016/j.quascirev.2014.03.018

Hijmans, R. J., Cameron, S. E., Parra, J. L., Jones, P. G., & Jarvis, A. (2005). Very high resolution interpolated climate surfaces for global land areas. *International Journal of Climatology*, *25*(15), 1965–1978. https://doi.org/10.1002/joc.1276

Huffman, G. J., Bolvin, D. T., Nelkin, E. J., Wolff, D. B., Adler, R. F., Gu, G., et al. (2007). The TRMM multisatellite precipitation analysis (TMPA): Quasi-global, multiyear, combined-sensor precipitation estimates at fine scales. *Journal of Hydrometeorology*, *8*(1), 38–55. https://doi.org/10.1175/JHM560.1

Hughes, P. D., & Gibbard, P. L. (2015). A stratigraphical basis for the last glacial maximum (LGM). *Quaternary International*, *383*, 174–185. https://doi.org/10.1016/j.quaint.2014.06.006

Jiang, D., Wang, H., & Lang, X. (2004). On the possibility of ice sheet over the Tibetan Plateau at the last glacial maximum (in Chinese). *Chinese Journal of Atmospheric Sciences*, *28*, 28–34.

Jouvet, G., Seguinot, J., Ivy-Ochs, S., & Funk, M. (2017). Modelling the diversion of erratic boulders by the Valais glacier during the last glacial maximum. *Journal of Glaciology*, *63*(239), 487–498. https://doi.org/10.1017/jog.2017.7

Kirchner, N., Greve, R., Stroeven, A. P., & Heyman, J. (2011). Paleoglaciological reconstructions for the Tibetan Plateau during the last glacial cycle: Evaluating numerical ice sheet simulations driven by GCM-ensembles. *Quaternary Science Reviews*, *30*(1–2), 248–267. https://doi.org/10.1016/j.quascirev.2010.11.006

Kuhle, M. (1985). Glaciation research in the Himalayas: A new ice age theory. *Universitas*, *27*, 281–294.

Kuhle, M. (1998). Reconstruction of the 2.4 million km^2 late Pleistocene ice sheet on the Tibetan Plateau and its impact on the global climate. *Quaternary International*, *45*, 71–108.

Liu, T., Zhang, X., Xiong, S., Qin, X., & Yang, X. (2002). Glacial environments on the Tibetan Plateau and global cooling. *Quaternary International*, *97*, 133–139.

Maussion, F., Scherer, D., Mölg, T., Collier, E., Curio, J., & Finkelnburg, R. (2014). Precipitation seasonality and variability over the Tibetan Plateau as resolved by the high Asia reanalysis. *Journal of Climate*, *27*(5), 1910–1927. https://doi.org/10.1175/JCLI-D-13-00282.1

Owen, L. A., & Dortch, J. M. (2014). Nature and timing of quaternary glaciation in the Himalayan–Tibetan orogen. *Quaternary Science Reviews*, *88*, 14–54. https://doi.org/10.1016/j.quascirev.2013.11.016

Owen, L. A., Finkel, R. C., Barnard, P. L., Haizhou, M., Asahi, K., Caffee, M. W., & Derbyshire, E. (2005). Climatic and topographic controls on the style and timing of Late Quaternary glaciation throughout Tibet and the Himalaya defined by ^{10}Be cosmogenic radionuclide surface exposure dating. *Quaternary Science Reviews*, *24*(12–13), 1391–1411. https://doi.org/10.1016/j.quascirev.2004.10.014

Owen, L. A., Finkel, R. C., & Caffee, M. W. (2002). A note on the extent of glaciation throughout the Himalaya during the global last glacial maximum. *Quaternary Science Reviews*, *21*(1–3), 147–157. https://doi.org/10.1016/S0277-3791(01)00104-4

RGI Consortium (2017). Randolph Glacier Inventory—A dataset of global glacier outlines: Version 6.0. Technical Report, Global Land Ice Measurements from Space, Colorado, USA.

Rupper, S., Roe, G., & Gillespie, A. (2009). Spatial patterns of Holocene glacier advance and retreat in Central Asia. *Quaternary Research*, *72*(03), 337–346. https://doi.org/10.1016/j.yqres.2009.03.007

Seong, Y. B., Owen, L. A., Bishop, M. P., Bush, A., Clendon, P., Copland, L., et al. (2007). Quaternary glacial history of the central Karakoram. *Quaternary Science Reviews*, *26*(25–28), 3384–3405. https://doi.org/10.1016/j.quascirev.2007.09.015

Shi, Y. (2002). Characteristics of late Quaternary monsoonal glaciation on the Tibetan Plateau and in East Asia. *Quaternary International*, *97*, 79–91.

Wang, P., Clemens, S., Beaufort, L., Braconnot, P., Ganssen, G., Jian, Z., et al. (2005). Evolution and variability of the Asian monsoon system: State of the art and outstanding issues. *Quaternary Science Reviews*, *24*(5–6), 595–629. https://doi.org/10.1016/j.quascirev.2004.10.002

Winkelmann, R., Martin, M. A., Haseloff, M., Albrecht, T., Bueler, E., Khroulev, C., & Levermann, A. (2011). The Potsdam parallel ice sheet model (PISM-PIK)—Part 1: Model description. *The Cryosphere*, *5*(3), 715–726. https://doi.org/10.5194/tc-5-715-2011

Xu, J., Grumbine, R. E., Shrestha, A., Eriksson, M., Yang, X., Wang, Y. U. N., & Wilkes, A. (2009). The melting Himalayas: Cascading effects of climate change on water, biodiversity, and livelihoods. *Conservation Biology*, *23*(3), 520–530. https://doi.org/10.1111/j.1523-1739.2009.01237.x

Xu, X. (2014). Climates during Late Quaternary glacier advances: Glacier-climate modeling in the Yingpu Valley, eastern Tibetan Plateau. *Quaternary Science Reviews*, *101*, 18–27. https://doi.org/10.1016/j.quascirev.2014.07.007

Yao, T., Thompson, L., Yang, W., Yu, W., Gao, Y., Guo, X., et al. (2012). Different glacier status with atmospheric circulations in Tibetan plateau and surroundings. *Nature Climate Change*, *2*(9), 663–667. https://doi.org/10.1038/nclimate1580

Yao, T., Thompson, L. G., Mosbrugger, V., Zhang, F., Ma, Y., Luo, T., et al. (2012). Third pole environment (TPE). *Environmental Development*, *3*, 52–64. https://doi.org/10.1016/j.envdev.2012.04.002

Yatagai, A., Kamiguchi, K., Arakawa, O., Hamada, A., Yasutomi, N., & Kitoh, A. (2012). APHRODITE: Constructing a long-term daily gridded precipitation dataset for Asia based on a dense network of rain gauges. *Bulletin of the American Meteorological Society*, *93*(9), 1401–1415. https://doi.org/10.1175/BAMS-D-11-00122.1